Proc. Natl. Acad. Sci. USA
Vol. 88, pp. 6810–6814, August 1991
Medical Sciences

Free magnesium levels in normal human brain and brain tumors: ^{31}P chemical-shift imaging measurements at 1.5 T

(^{31}P NMR spectroscopy/brain neoplasms/astrocytoma)

JUNE S. TAYLOR*†, DANIEL B. VIGNERON*, JOSEPH MURPHY-BOESCH*, SARAH J. NELSON*, HOWARD B. KESSLER‡, LARRY COIA§, WALTER CURRAN§, AND TRUMAN R. BROWN*

*Department of NMR and Medical Spectroscopy, ‡Department of Diagnostic Imaging, and §Department of Radiation Oncology, Fox Chase Cancer Center, Philadelphia, PA 19111

Communicated by Mildred Cohn, January 31, 1991

ABSTRACT **We have studied a series of normal subjects and patients with brain tumors, by using ^{31}P three-dimensional chemical shift imaging to obtain localized ^{31}P spectra of the brain. A significant proportion of brain cytosolic ATP in normal brain is not complexed to Mg^{2+}, as indicated by the chemical shift δ of the β-P resonance of ATP. The ATP β-P resonance position in brain thus is sensitive to changes in intracellular free Mg^{2+} concentration and in the proportion of ATP complexed with Mg because this shift lies on the rising portion of the δ vs. Mg^{2+} titration curve for ATP. We have measured the ATP β-P shift and compared intracellular free Mg^{2+} concentration and fractions of free ATP for normal individuals ($n = 6$) and a limited series of patients with brain tumors ($n = 5$). In four of the five spectra obtained from brain tissue containing a substantial proportion of tumor, intracellular free Mg^{2+} was increased, and the fraction of free ATP was decreased, compared with normal brain.**

Intracellular Mg^{2+} ($[Mg^{2+}]_i$) is a cofactor for many enzymes and signal-transduction proteins (1, 2) and strongly influences phosphorylation potentials. Nevertheless, as Corkey and coworkers point out (3), measurements of $[Mg^{2+}]_i$ are fewer and more disparate than those for other major biological cations. There is considerable evidence that $[Mg^{2+}]_i$ is actively transported and regulated, although the mechanisms responsible are largely unknown. The concentration of Mg^{2+} varies significantly from tissue to tissue. In striated muscle from a variety of animals, estimates of $[Mg^{2+}]_i$ range from 0.6 mM to 1.5 mM, and the percentage of ATP present as free ATP (ATP_f) is low (≈5%) (4–6). Measurements of $[Mg^{2+}]_i$ in perfused rat heart yield values of 0.8 mM (7, 8). In smooth muscle, however, ATP_f percentages of 15 to 25% are observed, corresponding to $[Mg^{2+}]_i$ from 0.2 mM to 0.5 mM (5, 9). $[Mg^{2+}]_i$ has been measured as 0.4–0.7 mM in rat liver (10, 11) and as ≈0.58–1.0 mM in rat brain (6, 10, 12); recently $[Mg^{2+}]_i$ equal to 0.3 mM has been reported for human brain (13) and guinea pig cerebral tissue (14).

The chemical shifts of the terminal phosphate resonances of ATP and ADP are influenced strongly by both pH and divalent cation concentration. The resonance shift of the β-P of ATP is affected primarily by divalent ion concentration and to a lesser degree by pH, temperature, and ionic strength (15). Because the predominant intracellular cation available for complexing cytosolic ATP is Mg^{2+}, shifts of the ATP β-P resonance from *in vivo* ^{31}P NMR spectra can be used to determine $[Mg^{2+}]_i$ (4).

To apply this method of measuring $[Mg^{2+}]_i$ to human brain, methods for obtaining spectra localized to the brain are needed. The localization method used in this study, three-dimensional chemical-shift imaging (3D-CSI), has the advantage of producing spectra from multiple volumes, or voxels, over the entire supratentorial volume of the brain (16). Obtaining spectra simultaneously from both normal and peritumoral regions of the brain in patients aids in the interpretation of the spectra from the tumor region(s). 3D-CSI-localized spectra also contain no chemical-shift artifact, which removes a possible source of bias in measurement of the ATP β-P chemical shifts relative to phosphocreatine (PCr) or other internal reference.

METHODS

Imaging/^{31}P Chemical-Shift Imaging (CSI) Spectroscopy. Combined proton imaging/^{31}P spectroscopic examinations of patients and healthy volunteers were done on a standard clinical imager [1.5 T Siemens (Iselin, NJ) Magnetom]. Positioning and proton imaging required 20 min; the $8 \times 8 \times 8$ 3D-CSI spectroscopic data required 17 min per two-acquisition block. For patients A, B, and C, ^{31}P spectra were acquired by using 5- or 10-cm-diameter ^{31}P surface coils and a 3D-CSI sequence with a sin/cos adiabatic half-passage pulse (17). For volunteers and patients D and E, spectra were acquired with a quadrature low-pass birdcage resonator and 3D-CSI with a 250-μs rectangular pulse with a low-tip angle as described (16); no spatial filtering was done. Retrospective alignment of the CSI voxels (16, 18) was used to position the voxels symmetrically with respect to the falx cerebri and to place the central axial slice below the corpus callosum for normal subjects. For patients B through E, a CSI voxel was centered on the tumor. For patient A, whose tumor contained large cystic regions, the CSI voxel was centered on the viable portion of the tumor, as assessed from Gd contrast-enhanced proton images. After shifting, the data were Fourier-transformed in time and k-space domains, and all spectra were phased with the same corrections (obtained from the nonlocalized spectrum) to produce a three-dimensional array of 512 spectra. The 3D-CSI spectra were corrected for the missing initial time points of the free induction decay (FID) (16, 19) to produce baseline-corrected spectra that are visually easier to inspect.

Patients. Three male and two female patients with brain tumors, aged 36–70 years, were examined. All examination procedures were approved by the Investigational Review Board. The histories of the patients were as follows: case A, recurrent oligodendroglioma in the left temporal lobe, treated

The publication costs of this article were defrayed in part by page charge payment. This article must therefore be hereby marked "*advertisement*" in accordance with 18 U.S.C. §1734 solely to indicate this fact.

Abbreviations: CSI, chemical-shift imaging; 3D-CSI, three-dimensional CSI; FID, free induction decay; PCr, phosphocreatine; $[Mg^{2+}]_i$, intracellular Mg^{2+}; ATP_f, free ATP; ISIS, image-selected *in vivo* spectroscopy; T_1 and T_2, longitudinal and transverse relaxation time, respectively.

†To whom reprint requests should be addressed at present address: Diagnostic Imaging Department, St. Jude Children's Research Hospital, Memphis, TN 38101.

3.5 yr previously with surgery, 45 Gy radiation, and chemotherapy; case B, glioblastoma multiforme in right temporal lobe, no treatment, examined 6 weeks after biopsy; case C, low-grade astrocytoma in left temporal lobe, examined after radiation therapy (36 Gy); case D, solitary metastasis to left frontoparietal lobe from squamous-cell lung carcinoma, examined 6 mo after radiation therapy (40 Gy); case E, bilateral hemispheric metastases from hepatoma, the largest being in the right occipital region, treated with multiple chemotherapeutic regimens and examined after initial fraction (3 Gy) of whole-brain radiation.

Calculations. Chemical shifts are expressed relative to 85 H_3PO_4 as 0 ppm. The brain PCr resonance was used as an internal reference (−2.52 ppm), unless otherwise noted.

pH titrations were done to determine δ for β-ATP at 37°C for solutions containing 150 mM KCl, 3 mM glycerophosphorylcholine, 3 mM PCr, 3 mM ATP, 3 mM P_i, and either 6 mM $MgCl_2$ or 5 mM cyclohexane diamine tetraacetic acid. The fraction of total ATP present as ATP_f was calculated as $\phi = [(d_{obs} - d_a)/(d_b - d_a)]$, where d_{obs} is δ observed, and d_a and d_b are the endpoint δ values for the β-P resonances of MgATP and ATP species, respectively, from the titrations; $d_a = -18.32$, and d_b ranged from −21.39 at pH 6.8 to −21.08 at pH 7.4. Values of pMg vs. observed β-P chemical shift at pHs of 7.0, 7.2, and 7.4 were computed from the relationship $pMg = pK' + \log[(d_a - d_{obs})/(d_{obs} - d_b)]$; pK′ for MgATP at 37°C was taken as 4.06 (11). pK′ for pHs other than 7.2 were corrected for pH as in ref. 20; an activity coefficient of 0.74 was used to compute $[H^+]$ (21).

RESULTS

Studies of Normal Subjects. Spectra from seven separate examinations on six volunteers (three males and three females, ages 21–43) were analyzed for ATP chemical shifts. Voxels located in the center and around the periphery of the cerebral hemispheres (Fig. 1*A*) were analyzed separately for each examination. Typical spectra are shown for the nonlocalized spectrum (Fig. 1*B*), a spectrum from a 27-cc volume in the brain, showing the rolling baseline artifacts resulting from the loss of seven initial time points of the FID (Fig. 1*C*), and the result of correcting for their absence (Fig. 1*D*). Corrected and uncorrected sets of spectra were analyzed for ATP chemical shifts in several exams. No significant difference in the ATP β-P means for corrected and uncorrected spectra was found ($P > 0.3$). The results presented here were based on analyses of uncorrected spectra.

Table 1 shows mean δ of the ATP β-P resonance of the central and peripheral brain voxels for each of the seven data sets, as well as the means for the volunteers as a group. For the signal/noise and spatial sampling (27-cc voxels) of this data, no difference in β-P chemical shift between central and peripheral volumes was observed ($P > 0.3$). The population mean and SEM for the β-P chemical shift were −19.02 ± 0.017 ppm, significantly upfield from the position of this resonance in skeletal muscle (−18.4 to −18.5).

Like the β resonance, the γ resonance of ATP also shifts upfield as the fraction of ATP complexed to Mg^{2+} decreases, albeit less than the β resonance. When the ATP γ-P chemical shifts are plotted vs. β-P shifts for individual spectra, the spectra arising from voxels composed of brain or primarily of skeletal muscle indeed fall into two groups. Taking data set 1A as an example, the mean shift and SEM for the ATP β-P resonance for muscle voxels, −18.45 ± 0.08 ppm ($n = 3$), agrees well with values previously observed for skeletal muscle (4, 6), whereas the mean shift for the brain voxels plotted for this data set was −18.92 ± 0.05 ($n = 13$). The γ-P mean shifts were −4.80 ± 0.06 ppm ($n = 3$) and −5.25 ± 0.030 ($n = 13$) for muscle and brain voxels, respectively.

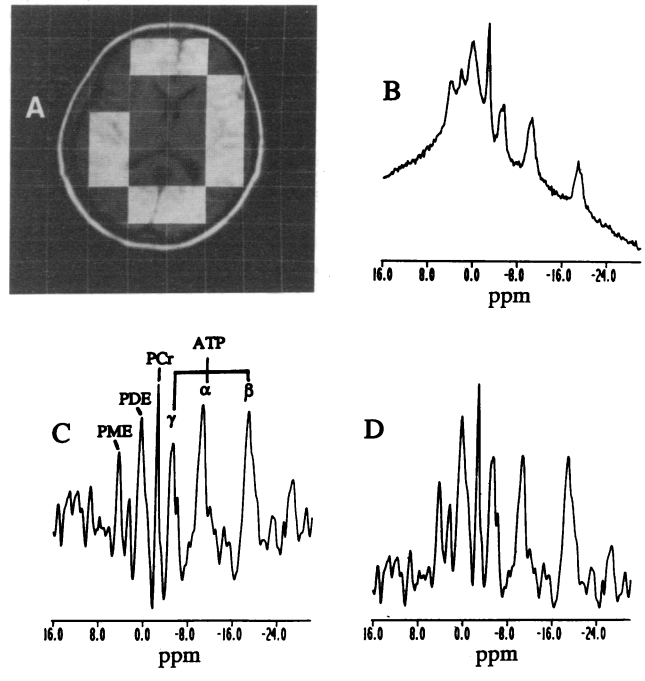

FIG. 1. ^{31}P *in vivo* spectra of normal human brain. (*A*) Axial longitudinal relaxation time (T_1)-weighted proton image of normal brain, overlaid with shifted spectral sampling grid. Spectra from deep-lying central localized volumes (voxels) and from more peripheral voxels were analyzed separately for ATP β-P chemical shifts. Highlighted areas show peripheral voxels, enclosing the central voxels. All spectral data were collected with repetition time (TR) = 1 s, spectral width = 2 kHz, and 256 or 512 data points in the time domain and zerofilled to 512 time points. (*B*) Nonlocalized FID acquired with ^{31}P birdcage coil as described. The FID was zerofilled to 512 points; no filtering was applied. (*C*) Spectrum localized to 27-cc voxel in brain, from 3D-CSI data set with eight acquisitions per phase encode step. A Lorentzian filter of 15 Hz was applied in the time domain, and the first 3.1 msec of data was zeroed. (*D*) Spectrum in *C*, after correction for missing early time points of the FID. PME, phosphomonoester; PDE, phosphodiester.

The observed ATP β-P chemical shift for human brain in our normal population was −19.02 ppm; the SD for shifts computed for individuals was ≈0.2 ppm. The mean β-P shift corresponds to 76% ATP existing in solution as the Mg complex in equilibrium with 24% ATP and with 0.35 ± 0.01 mM free Mg^{2+}. In contrast, in the muscle spectra of data set 1A, 96% of the ATP was bound to Mg, and the free $[Mg^{2+}]$ was >1 mM.

Patient Studies. Five patients with tumors >1.5-cm diameter and volumes ranging from 4 to 94 cc were studied. The

Table 1. ATP β-P ^{31}P chemical shifts in brains of healthy subjects

Subject	Central β-P shift, mean ppm ± SEM (n)	Peripheral β-P shift, mean ppm ± SEM (n)
1A*	−19.05 ± 0.05 (9)	−18.87 ± 0.06 (10)
1B	−19.03 ± 0.09 (10)	−18.94 ± 0.06 (10)
2	−19.12 ± 0.10 (10)	−19.11 ± 0.03 (5)
3	−18.94 ± 0.04 (10)	−19.04 ± 0.05 (8)
4	−19.04 ± 0.07 (8)	−19.00 ± 0.04 (8)
5	−19.14 ± 0.03 (9)	−19.14 ± 0.05 (14)
6	−18.96 ± 0.03 (8)	−18.99 ± 0.05 (9)
Mean	−19.04 ± 0.027	−19.01 ± 0.021
Population mean†	−19.02 ± 0.017 (128)	

*In the first four examinations, four acquisitions per phase encode were collected; for the second three examinations, eight acquisitions per phase encode were collected.
†Population mean is a cumulative (central and peripheral) mean.

first patients (A, B, and C) were examined by using surface coils. The surface-coil studies provided a small number of suitable spectra limited to the region of the brain superficial to and including tumor, which lay within 6 cm of the surface of the temporal lobe in these patients. Examinations of patients D and E were done with the ^{31}P birdcage; in these cases, spectra were obtained from both cerebral hemispheres.

Fig. 2 shows the spectra from the tumor-containing voxels for the five patients. All spectra from tumor-containing regions show a marked reduction in PCr, compared with spectra from normal brain (Fig. 1*C*), whereas ATP is maintained at nearly normal levels. The P_i and phosphomonoester region are obviously elevated in some, but not all, cases. Table 2 shows ATP β-P shifts, pH, $[Mg^{2+}]_i$, and the ATP_f calculated for the voxel localized to tumor in the five patients. As a group, the ATP β-P resonance in the *in vivo* spectra arising primarily or partially from these brain tumors [mean, SEM = -18.76 ppm $\pm$ 0.08 (n = 5)] appears downfield from the β-resonance position in the normal subjects. In those cases for which we have full three-dimensional volume data (patients D and E), the largest downfield shifts for the β-P were limited to the region of tumor tissue and/or one adjacent voxel and did not extend over the surrounding edematous tissue. In calculating ATP_f and $[Mg^{2+}]_i$, it is necessary to know the tissue pH because of its effect on both the K_d and the endpoint, d_b, of the titration curve (22). Tumor-tissue pH was calculated or estimated for the tumor spectra, as noted in Table 2, and these pH values were used in calculating columns 4 and 5.

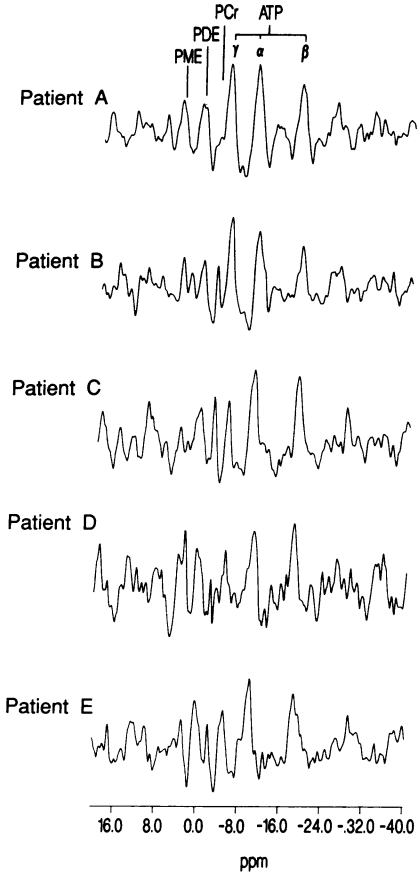

FIG. 2. ^{31}P spectra localized to tumor and peritumoral brain. Spectra localized to tumor for patient A (48-cc voxel), patient B (27-cc voxel), patient C (48-cc voxel), and patients D and E (27-cc voxel).

Table 2. ATP β-P chemical shifts and $[Mg^{2+}]_i$ from tumor voxels in human brain

Patient	Shift, ppm	pH*	$[Mg^{2+}]$, mM	ATP_f, %
A†	−18.78	7.00	0.58	16
B‡	−18.78	7.32	0.41	17
C†	−18.75	7.00	0.63	15
D‡	−18.50	7.15	1.3	6
E‡	−19.00	7.25	0.24	25

For patients A and E, the tumor constituted >95% of the voxel volume; for patients B, C, and D tumor volume ranged from 16–36% of the voxel volume.

*For patients B, D, and E, pH was determined from the peak position of the P_i resonance in the tumor voxel. For patients A and C, pH was taken to be normal brain pH (7.00).

†CSI voxel volume equals 48 cc.

‡CSI voxel volume equals 27 cc.

Fig. 3*A* is a fast transverse relaxation time (T_2)-weighted proton image of an axial slice through patient D's tumor, showing the tumor and surrounding region of edema. The CSI data was shifted to center one voxel on the tumor, which represents ≈36% of voxel volume (Fig. 3*B*). Fig. 3*C* shows spectra from voxels corresponding to those highlighted in Fig. 3*B*, with the box indicating the tumor. Inspection of the spectra shows that PCr was essentially zero in the tumor voxel, but ATP was only slightly reduced. The phosphomonoester peak region and P_i were elevated in the tumor and in voxels surrounding the tumor. The pH was significantly alkaline in the voxels anterior and posterior to the tumor.

Taking pH into account, $[Mg^{2+}]_i$ values for the regions of patient D's brain anterior and posterior to tumor were 0.21 and 0.28 mM, respectively. The mean $[Mg^{2+}]_i$ level ($\pm$ SD) in

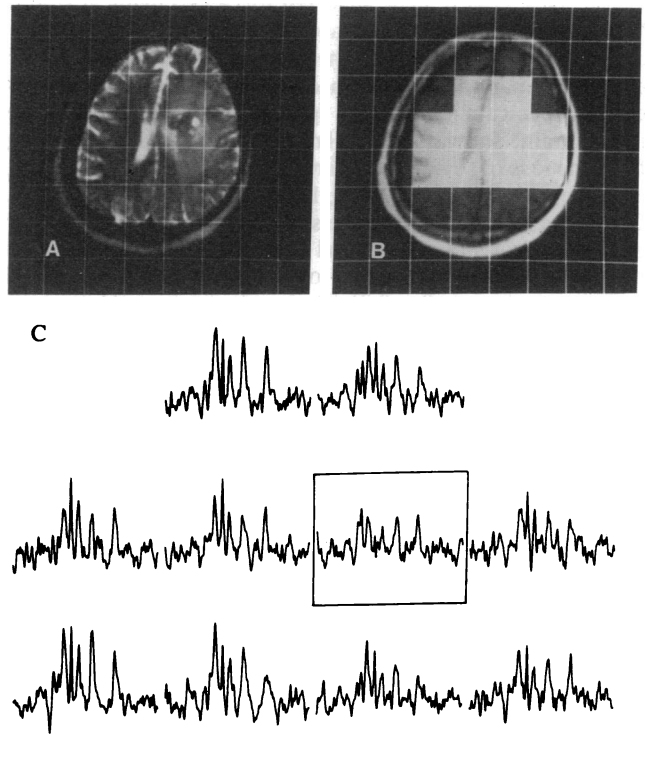

FIG. 3. ^{31}P spectra from tumor region and surrounding brain for patient D. (*A*) Axial steady-state free precession (PSIF) image, showing tumor and edema and shifted sampling grid. Sequence parameters: α = 70°, repetition time (TR) = 30 ms, echo time (TE) = 11 ms. (*B*) Axial T_1-weighted proton image with highlighted voxels corresponding to spectra in *C*. (*C*) Spectra from region highlighted in *B*. Filtering was 15 Hz Lorentzian in time domain.

the voxels surrounding the tumor in the left hemisphere is 0.36 ± 0.10 ($n = 10$), and in the contralateral hemisphere the $[Mg^{2+}]_i$ level is 0.40 ± 0.24 ($n = 11$). Because PCr was not observed in the tumor voxel, two other methods of referencing chemical shifts were used. (*i*) The tumor was assumed to have the same susceptibility as the surrounding tissue, and therefore chemical shifts in the tumor were referenced to the PCr resonance frequency of the surrounding tissue. This method resulted in an ATP β-P shift in the tumor voxel of -18.50 ppm and a P_i shift of 2.49, corresponding to pH = 7.15. (*ii*) The α-ATP resonance was used as the chemical-shift reference and set to the mean value for the nontumor voxels in this brain, -10.39 ppm ($n = 21$). This technique resulted in a β-P shift in the tumor of -18.30, whereas P_i was 2.69, corresponding to a pH of 7.34. In any event, the β-P shift in the tumor voxel is ≤ -18.50, so that $[Mg^{2+}]_i$ in the tumor and peritumoral region is ≥ 1.3 mM, which is elevated by ≥ 4 SD above the $[Mg^{2+}]_i$ levels in surrounding brain. $[Mg^{2+}]_i$ is also elevated in the voxel to the right of the tumor.

Patient E's major metastasis represented 95% of the voxel and was surrounded by an extensive region of edema. PCr was greatly reduced in the tumor voxel, but ATP was not reduced (data not shown). P_i was elevated in the tumor; pH was alkaline (>7.2) in and anterior to the tumor. Elevated P_i and pH were also observed near one of the smaller metastases in the contralateral hemisphere. The ATP β-P shift in the spectrum from the tumor-containing voxel was identical to the mean shift for normal brain. In this case, the spectrum from the voxel anterior to the tumor showed the greatest downfield shift, -18.53 ppm, corresponding to $[Mg^{2+}]_i = 0.99$ mM.

To compare these data, we constructed histograms of the distributions for the normal population of Table 1 (Fig. 4*A*), and for patients D and E, including the tumor voxel (in black) (Figs. 4 *C* and *D*, respectively). The mean shifts ($\pm$ SEM) for the patient distributions are -18.98 ± 0.04 ($n = 22$) for patient D and -18.98 ± 0.04 ($n = 23$) for patient E. These mean values are normal in relation to 4*A* ($P > 0.25$). Fig. 4*B* presents the distribution for the five tumor observations, with a mean shift and SEM of 18.76 ± 0.08 ($P < 1.005$). In summary, the ATP β-P shifts from the regions containing tumor were at the extreme downfield end of the normal distribution for four of the five tumors observed to date.

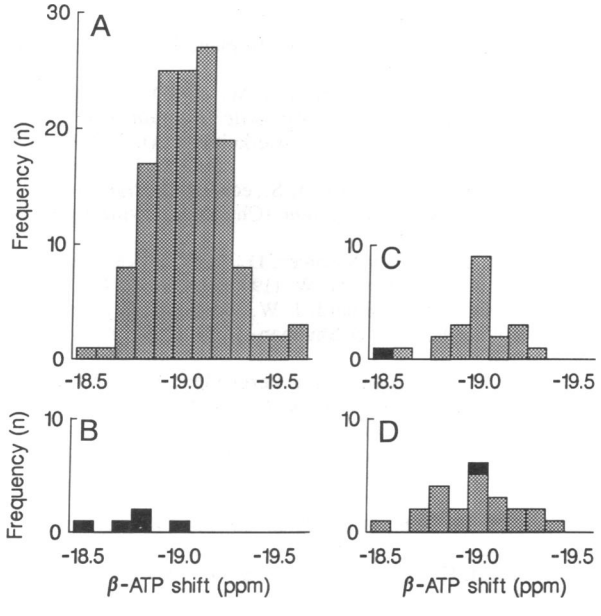

FIG. 4. Histograms of ATP β-P chemical shifts. (*A*) ATP β-P shifts from 3D-CSI spectra localized to brains of normal volunteers ($n = 138$). (*B*) Shifts for the five spectra localized to tumor for patients A–E. (*C*) Shifts from 3D-CSI spectra localized to brain of patient D ($n = 22$); tumor shift in black. (*D*) Shifts for patient E ($n = 23$); tumor shift in black.

DISCUSSION

The $[Mg^{2+}]_i$ and ATP β-P chemical shift values for our normal human population may be compared with recent $[Mg^{2+}]_i$ determinations in humans (13) and animals (23, 24) and *in vivo* shift determination of Hubesch and coworkers (25), respectively. Ramadan *et al.* (13) used topical magnetic resonance localization to study magnesium levels in the brains of normal subjects and patients suffering from migraine. Their observed $[Mg^{2+}]_i \pm$ SEM for normal subjects was 0.30 ± 0.01 mM. Interestingly, they found $[Mg^{2+}]_i$ to be reduced in patients during a migraine attack, whereas intracerebral pH remained normal during the attack. The shifts of the P_i peaks seen in our normal brain spectra correspond to pH from 6.95 to 7.05, in excellent agreement with pH values previously observed in normal brain (13, 25, 26). Our mean values for $[Mg^{2+}]_i$ are also in excellent agreement with the values of 0.4 mM obtained for *in vivo* mammalian brain (23) and 0.33 mM obtained for superficial rodent cerebral tissue (14).

Hubesch *et al.* (25) reported metabolite concentrations and chemical shifts for *in vivo* ^{31}P spectra from a normal population and 13 brain tumor patients studied with image-selected *in vivo* spectroscopy (ISIS). The ATP β-P shift for 13 normal controls was reported to be -18.77 ± 0.04 ppm, and the P_i shift was 2.33 ± 0.02 (converted to reference PCr as -2.52 ppm). Chemical shifts from the tumor population were not reported in this study. The P_i shift is in satisfactory agreement with the corresponding value from our study, 2.27 ± 0.05 ppm ($n = 7$). However, the reported shift for β-P is significantly downfield from our value. The major differences between this study and the work reported here are in size of the localized volume (125 cc in the study of Hubesch *et al.* and 27 cc in our work) and the technique used to localize the volume (ISIS vs. 3D-CSI in our work). One possible reason for the discrepancy in the two studies is a more significant contamination from surface muscle tissue for the β-P peak in the ISIS study. This contamination could arise for two reasons: either contamination due to imperfect cancelation of signals from outside the volume or from the fact that the β peak comes from a different region than the PCr peak, due to the chemical-shift displacement of the respective ISIS voxels. Because neither the selective pulse band widths nor the gradient strengths were given in ref. 25, it was not possible to calculate the distance the voxels were shifted with respect to each other. In analogous experiments, gradient strengths corresponded to an offset of at least 1 cm (out of 5-cm voxel dimension) between the PCr and β-P voxels (27). Because the voxels are shifted relative to each other in all three dimensions, only 51% ($4^3/5^3$) of the volume is in common between the PCr and β-P voxels. This difference in volumes of localization for ATP β-P and PCr resonances appears substantial enough to account for the differences between studies.

In normal subjects, brain $[Mg^{2+}]_i$ and fractions of free ATP appear reproducible, indicating some active mechanism for maintenance of this low $[Mg^{2+}]_i$. Normal serum mean Mg levels are 0.7–1.0 mM in humans, of which 55% is free Mg^{2+} (2). In the central nervous system, total Mg concentrations in the cerebrospinal fluid are maintained at 1.0–1.2 mM, of which 55% is the free ion; this is so even for severe hypermagnesemia, in which serum levels rise three to five times normal (2). In brain, if $[Mg^{2+}]_i$ and extracellular Mg^{2+} were in equilibrium with a membrane potential of -65 mV (44), $[Mg^{2+}]_i$ would be ≈ 65 mM. The free $[Mg^{2+}]_i$ we observe in normal brain is more than two orders of magnitude lower than this. This fact implies the

existence of a mechanism for net transport of Mg^{2+} out of the cells.

The low levels of $[Mg^{2+}]_i$ we have seen in normal brain suggest a possible significance for ATP_f levels. Total cytosolic NTP, most of which is ATP, varies greatly from one tissue to another: 1.85 mM for smooth muscle (5), 2–2.7 mM in human liver (28), 3 mM in human brain (25, 27, 29), 6.8 mM in rat heart (5, 7), and 7 mM in human skeletal muscle (30). In the same tissues, the ATP_f level shows much less variation: 0.28–0.31 mM in smooth muscle (5, 9), 0.35 mM in rat heart (5, 7), 0.4 mM in liver (11), and 0.4 mM in skeletal muscle (30). In human brain, our results indicate ATP_f = 0.6–0.7 mM in normal brain and 0.3–0.4 mM in tumor-containing tissue. It is clear from numerous studies that the relationship between $[Mg^{2+}]_i$, total cytosolic ATP, and ATP_f is subject to both acute and long-term changes, in response to physiological and pathological processes. However, the greater consistency of ATP_f, compared with total ATP or $[Mg^{2+}]_i$, points to a possible significance for ATP_f in this regulatory network. ATP_f has been shown to be an inhibitor in a number of important reactions (31, 32).

In our patients, higher levels of $[Mg^{2+}]_i$ were observed in the localized volumes containing or immediately adjacent to the tumors. Increases in brain $[Mg^{2+}]_i$ of similar magnitude have been shown, consequent to severe ATP depletion (to <50% of control levels) induced by hypoglycemia (23). However, in the present study the increase in $[Mg^{2+}]_i$ cannot be attributed simply to decreases in ATP content because ATP levels were not severely or selectively decreased in the volumes where $[Mg^{2+}]_i$ was elevated. In contrast, PCr was drastically and selectively lowered in tumor-containing volumes. The relaxation times for the phosphorus metabolites in the region of tumor and edema are not known, but the drop in PCr is too great to be explained solely by altered T_1 values. The effects in tumor regions resembled closely the increases in $[Mg^{2+}]_i$, with maintenance of ATP levels and lowered PCr, in guinea pig cerebral tissue subjected to hypoxic conditions (14). Interestingly, an earlier study of superfused excised breast tumor tissue (33) showed 15% ATP_f in malignant tumors, a fraction comparable to those in the final column of Table 2. However, in that study (33) benign tumors were found to have a substantially lower fraction of free ATP (5%), indicating a level of $[Mg^{2+}]_i$ comparable to that found in skeletal muscle.

Our preliminary data show evidence for significant ATP β-P shifts associated with the presence of tumor. The tumor voxels also showed the greatest decrease in PCr. In contrast, more modest decreases in ATP, increases in the phosphomonoester peak region, and alkaline pH, expressed in the P_i-resonance shift, were observed in a wider surrounding peritumoral region, as well as in the tumor voxel. These early results show that 3D-CSI ^{31}P spectroscopy can visualize regions of abnormal metabolism in the peritumoral regions of the brain for tumor patients and can provide simultaneous evaluations of several metabolites, such as intracellular Mg^{2+}, pH, and the energy metabolites PCr, P_i, and ATP. The three-dimensional volume data contain sufficient information to assess multiple anomalous regions—e.g., tumor or regions of edema, against the background of the remaining voxels, in effect using the patient as his own control. The extent and nature of physiological abnormalities associated with brain tumors or other pathologies may thus be more completely defined.

We thank Tamela Willard, Edward Kosinski, Radka Stoyanova, Titia Scherpbier-Heddema, and James Hildenberger for excellent technical assistance, and Dr. Sam Litwin for valuable discussions. This work was supported by National Institute of Health Grants CA49516 (J.S.T.), CA41078 (T.R.B.), and CA06927 (to Fox Chase Cancer Center).

1. Grubbs, R. D. & Maguire, M. E. (1987) *Magnesium* **6**, 113–127.
2. Elin, R. J. (1987) *Clin. Chem.* **33**, 1965–1970.
3. Corkey, B. E., Duszynski, J., Rich, T. L., Matschinsky, B. & Williamson, J. R. (1986) *J. Biol. Chem.* **261**, 2567–2574.
4. Gupta, R. K., Gupta, P., Yushok, W. & Rose, Z. B. (1983) *Physiol. Chem. Phys. Med. NMR* **15**, 265–280.
5. Kushmerick, M. J., Dillon, P. F., Meyer, R. A., Brown, T. R., Krisanda, J. M. & Sweeney, H. L. (1986) *J. Biol. Chem.* **261**, 14420–14429.
6. Adam, W. R., Craik, D. J., Hall, J. G., Kneen, M. M. & Wellard, R. M. (1986) *Magn. Reson. Med.* **7**, 300–310.
7. Headrick, J. P. & Willis, R. J. (1989) *Magn. Reson. Med.* **12**, 328–338.
8. Murphy, E., Steenbergen, C., Levy, L. A., Raju, B. & London, R. E. (1989) *J. Biol. Chem.* **264**, 5622–5627.
9. Degani, H., Shafer, A., Victor, T. A. & Kaye, A. M. (1984) *Biochemistry* **23**, 2572–2577.
10. Veloso, D., Gwynn, R., Oskarsson, M. & Veech, R. L. (1973) *J. Biol. Chem.* **248**, 4811–4819.
11. Malloy, C. R., Cunningham, C. C. & Radda, G. K. (1986) *Biochim. Biophys. Acta* **885**, 1–11.
12. Vink, R., McIntosh, J. K., Demediuk, P., Weiner, M. W. & Faden, A. I. (1988) *J. Biol. Chem.* **263**, 757–761.
13. Ramadan, N. M., Halvorsen, H., Vande-Linde, A., Levine, S. R., Helpern, J. A. & Welch, K. M. A. (1989) *Headache* **29**, 416–419.
14. Brooks, K. J. & Bachelard, H. S. (1989) *J. Neurochem.* **53**, 331–334.
15. Cohn, M. & Hughes, T. R., Jr. (1962) *J. Biol. Chem.* **237**, 176–181.
16. Vigneron, D. B., Nelson, S. J., Murphy-Boesch, J., Kelley, D. A. C., Kessler, H. B., Brown, T. R. & Taylor, J. S. (1990) *Radiology* **177**, 643–649.
17. Brown, T. R., Buchthal, S. B., Murphy-Boesch, J., Nelson, S. J., Taylor, J. S. & Thoma, W. T. (1989) *J. Magn. Reson.* **82**, 629–633.
18. Gonzalez, R. & Wintz, C. (1977) *Digital Image Processing* (Addison–Wesley, Reading, MA), pp. 36–53.
19. Nelson, S. J. & Brown, T. R. (1991) *Bull. Magn. Reson.* **13**, in press.
20. O'Sullivan, W. J. & Smithers, G. W. (1979) *Methods Enzymol.* **63**, 294–336.
21. Tsien, R. Y. & Rink, T. J. (1980) *Biochim. Biophys. Acta* **599**, 623–638.
22. Phillips, R. C., George, P. & Rutman, R. J. (1966) *J. Am. Chem. Soc.* **88**, 2631–2640.
23. Petroff, O. A. C. & Prichard, J. W. (1987) in *Sixth Annual Meeting of the Society of Magnetic Resonance in Medicine* (Soc. Magnet. Reson. Med., Berkeley, CA), Vol. 2, p. 527 (abstr.).
24. McIlwain, H. & Bachelard, H. S., eds. (1985) *Biochemistry and the Central Nervous System* (Churchill Livingstone, New York), 5th Ed.
25. Hubesch, B., Sappey-Marinier, D., Roth, K., Meyerhoff, D., Matson, G. & Weiner, M. W. (1990) *Radiology* **174**, 401–409.
26. Petroff, O. A. C., Prichard, J. W., Behar, K. L., Alger, J. R., den Hollander, J. A. & Shulman, R. G. (1985) *Neurology* **35**, 781–788.
27. Luyten, P. R., Groen, J. P., Vermeulen, J. W. A. H. & den Hollander, J. A. (1989) *Magn. Reson. Med.* **11**, 1–21.
28. Meyerhoff, D. J., Boska, M. D., Thomas, A. M. & Weiner, M. J. (1989) *Radiology* **173**, 393–400.
29. Bottomley, P. A. & Hardy, C. J. (1989) *Clin. Chem.* **35**, 392–395.
30. Wray, S. & Tofts, P. S. (1986) *Biochim. Biophys. Acta* **886**, 399–405.
31. Bachelard, H. S. & Goldfarb, P. S. G. (1969) *Biochem. J.* **112**, 579–586.
32. Jangaard, N. O., Unkeless, J. & Atkinson, D. E. (1968) *Biochim. Biophys. Acta* **151**, 225–235.
33. Degani, H., Horowitz, H. & Itzeliak, Y. (1986) *Radiology* **161**, 53–55.